NUKLEONIKA 2003;48(Supplement 1):S41–S44

^{57}Fe Mössbauer spectroscopy and X-ray diffraction study of gadolinites $REE_2Fe^{2+}Be_2Si_2O_{10}$ from Lower Silesia (Poland) and Ytterby (Sweden)

Dariusz Malczewski

Abstract This paper reports the results of ^{57}Fe Mössbauer spectroscopy, X-ray diffraction (XRD) and gamma-ray spectroscopy studies of partially metamict gadolinites from Szklarska Poręba and Zimnik (Lower Silesia, Poland), a fully metamict gadolinite sample from Ytterby (Sweden) and a crystalline sample obtained after annealing of a fragment of the sample from Ytterby at 1373 K in an argon atmosphere. Both fully metamict and crystalline gadolinite show divalent iron exclusively in octahedral coordination. Changes of the amplitudes ratio of high energy to low energy absorption peaks from Fe^{2+} quadrupole doublets are strictly correlated with calculated absorbed alpha-dose and the metamictization stages of the gadolinite specimens. In this respect, one of the samples is in conflict with the estimated radiation dose based on age and radionuclide concentrations. In this case, Mössbauer spectroscopy shows that the sample had to be naturally annealed over geologic time.

Key words gadolinite • Mössbauer spectroscopy • X-ray diffraction • α-decays

Introduction

Metamict minerals are a class of natural amorphous materials, which were initially crystalline. Metamict minerals contain uranium and thorium. They are optically isotropic, X-ray amorphous, and their crystalline structure can be reconstituted by annealing. The mechanism for the transition from crystalline to amorphous structure is not quite understood [9] but the progressive overlap of recoil nuclei collision cascades from α-decay of ^{238}U, ^{232}Th, ^{235}U and their daughter products is critical to the process [1, 2]. Investigations of these materials are important because natural minerals containing large concentrations of U and Th can serve as natural analogues for radiation effects in high-level nuclear waste (HLW) forms [7, 14]. Gadolinite $REE_2Fe^{2+}Be_2Si_2O_{10}$, where REE means rare earth elements and yttrium, is commonly found in the fully or partially metamict state. The basic structure of gadolinites consists of sheets of SiO_4 and BeO_4 tetrahedrons interconnected by layers of distorted octahedral iron and 8-coordinate yttrium, rare earth elements and actinides (U and Th) [3, 8].

Samples characterization

The investigated gadolinite samples are from pegmatites of Ytterby, Sweden (GYT) Szklarska Poręba, Poland (GSP, GSPKM) and Zimnik, Poland (GZI). The sample from Ytterby is fully metamict, pitch black and resembles a piece of glass. The sample GSPKM is black, heavily fractured and rimmed by iron hydroxide. Despite the same localization, the GSP sample exhibits a degree of metamictization different from that of GSPKM, and is not black but dark

D. Malczewski
Faculty of Earth Sciences,
University of Silesia,
60 Będzińska Str., 41-200 Sosnowiec, Poland,
Tel.: +48 32/ 291 83 81 ext. 316, Fax: +48 32/ 291 58 65,
e-mail: malczews@us.edu.pl

Received: 17 July 2002, Accepted: 12 December 2002

Table 1. Ages, Fe, U and Th contents and calculated absorbed α-dose of gadolinite samples.

	GYT	GSP	GSPKM	GZI
Age (years)	$1795(2) \times 10^{6}$[a]	$328(12) \times 10^{6}$[b]	$328(12) \times 10^{8}$[b]	$280(12) \times 10^{8}$[c]
FeO (wt.%)[d]	13.54(2)	12.04(2)	12.42(2)	9.56(2)
U (wt.%)[e]	0.18(2)	0.42(2)	0.04(1)	0.20(2)
Th (wt.%)[e]	0.84(2)	1.24(4)	1.27(3)	0.47(5)
Calculated dose (α-decay/mg)[e]	$2.4(1) \times 10^{6}$	$7.7(3) \times 10^{15}$	$3.7(1) \times 10^{15}$	$2.8(2) \times 10^{15}$

[a]Ref. [10]. [b]Ref. [11]. [c]Ref. [12]. [d]Ref. [4]. [e]Ref. [5].

grey without traces of iron hydroxides or oxides. The Zimnik specimen is a black, broken crystal fragment associated with muscovite, quartz and microcline [4]. Some characteristics of these samples are given in Table 1, which shows that iron is an important constituent of the presented gadolinites with a content ranged from 9.56 to 13.54 wt.% [4]. Based on the ^{238}U and ^{232}Th concentrations the values of the absorbed α-dose D (Table 1) have been calculated from the equation:

$$(1) \qquad D = 8 \cdot N_{238} \, (e^{t \cdot \lambda 238} - 1) + 6 \cdot N_{232} \, (e^{t \cdot \lambda 232} - 1)$$

where: D is the absorbed dose (α-decay/mg), N_{238} and N_{232} are the present numbers of atoms ^{238}U and ^{232}Th per milligram, λ_{238}, λ_{232} are the decay constants of ^{238}U and ^{232}Th, t is the geologic age.

Experimental

The samples were powdered and prepared in the shape of a thin disc absorber (thickness 5 mg Fe/cm^2). The Mössbauer transmission spectra were recorded at room temperature using a constant acceleration spectrometer with triangular velocity shape, a multichannel analyzer with 1024 channels, and a linear arrangement of a ^{57}Co/Cr source (= 50 mCi), absorber and detector. The concentrations of ^{232}Th and ^{238}U were calculated from the count rates of the γ-ray transitions from ^{228}Ac, ^{226}Ra, ^{214}Pb, ^{214}Bi and ^{208}Tl, with ^{226}Ra (100 Bq) efficiency calibration source using a Ge(Li) detector. The samples were also examined by X-ray powder diffraction (XRD) using a fully automated SIEMENS D5000 diffractometer in the (Θ–Θ) system and CuK_{α_1} = 1.5406×10^{-10} m radiation.

Results and discussion

The Mössbauer spectra and XRD-patterns of the four gadolinites studied are shown in Fig. 1, and the parameters derived from the fitting procedure are summarized in Table 2. There is good agreement between the results from Mössbauer spectroscopy and XRD (Fig. 1); the Mössbauer lines are more broadened for the less crystalline samples. This observation enables connection between the experimental parameter $(B - I_H)/(B - I_L)$ defined from Fig. 2, and the increase of crystallinity and absorbed α-dose for the examined samples. The main feature seen in the Mössbauer spectrum of GYT (Fig. 1) is the presence of two asymmetric and broadened resonance – absorption peaks. Broadening of the spectral lines indicates the presence of numerous somewhat different positions of iron ions. The corresponding quadrupole splitting distribution (QSD) [5], using MOS MOD 8.2 code [13], is continuous with two maxima at 1.670(6) mm/s and 2.14(1) mm/s (average value of quadrupole splitting QS_{av} = 1.902 mm/s). These QS maxima are clearly separated at QS = 1.80 mm/s and the integral of the areas under the 1.67 and 2.14 mm/s peaks are 0.44 and 0.56, respectively. It is worth noting that the calculated average isomer shift (IS) for this QSD, IS_{av} =

Table 2. Parameters of ^{57}Fe Mössbauer spectra (Fig. 1) of the gadolinite samples. Isomer shift values (IS) are given relative to the α-Fe standard at room temperature. The linewidth of the standard is Γ_s = 0.142(2) mm/s. The errors are given from fitting procedure using the MOS MOD 8.2 and MEP code.

Sample	Doublet no.	χ^2	IS (mm/s)	QS (mm/s)	Γ[a] (mm/s)	Assignment (CN)[b]	Intensity (%)
GYT*		1.315	1.036(7)	1.902(4)	0.31(1)[c]	Fe^{2+} (6)	49.9
					0.43(1)[d]		50.1
GSPKM	1	1.294	1.004(7)	1.57(2)	0.21(2)	Fe^{2+} (6)	16.1
	2		1.091(3)	2.10(1)	0.29(1)	Fe^{2+} (6)	58.8
	3		0.370(1)	1.32(2)	0.42(2)	Fe^{3+} (6)	25.1
GZI	1	1.018	1.032(3)	1.64(2)	0.19(1)	Fe^{2+} (6)	53.3
	2		1.058(5)	1.99(5)	0.25(1)	Fe^{2+} (6)	46.7
GSPKM	1	1.320	1.040(1)	1.779(3)	0.222(2)	Fe^{2+} (6)	100
GYT-CR	1	0.834	1.041(1)	1.690(1)	0.186(2)[c]	Fe^{2+} (6)	50.6
					0.150(1)[d]		49.4

*Average values from QSD fitting. [a]Half widths at half maximum. [b]Coordination number.
[c]Low energy peak Γ_L. [d]High energy peak, Γ_H.

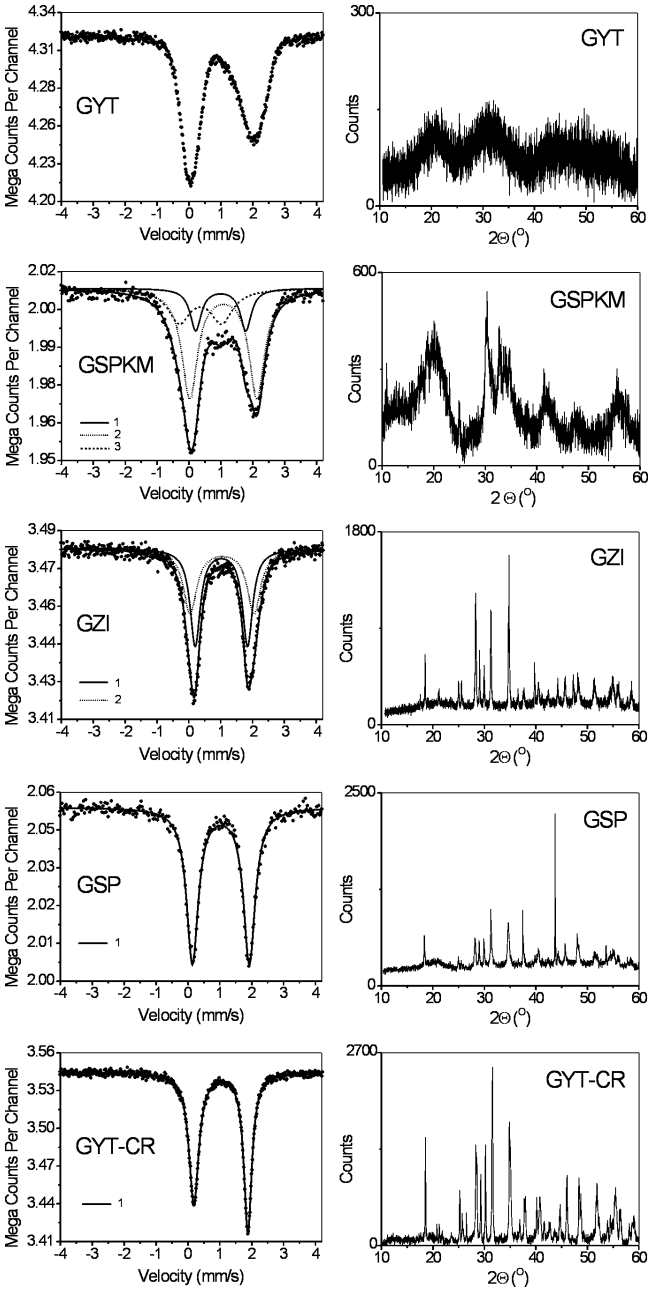

Fig. 1. ^{57}Fe Mössbauer spectra of GYT, GSPKM, GZI, GSP and GYT-CR samples. Solid dots – experimental data; thick solid line – fitted curve; thin solid line – doublet no. 1 (Fe^{2+}); dotted line – doublet no. 2 (Fe^{2+}); dashed line – doublet no. 3 (Fe^{3+}) (left side); corresponding XRD patterns (right side).

= 1.036 mm/s (Table 2) has nearly an identical value, in the range of uncertainty, as in the crystalline phase of gadolinite (Fig. 1, Table 2), where IS = 1.041 mm/s. It means that in the metamict state of gadolinite the positions reserved for iron are occupied exclusively by Fe^{2+} ions in octahedral coordinations only. The GSPKM sample is nearly metamict (amorphous). Its Mössbauer spectrum shows two quadrupole doublets (no. 1 and 2 in Fig. 1) assigned to Fe^{2+} at the octahedral sites strongly altered during metamictization, and one quadrupole doublet assigned to Fe^{3+} (no. 3 in Fig. 1) from the fragment of oxidized surface of this specimen. The GZI sample is partially metamict and its Mössbauer spectrum can be fitted by two Fe^{2+} quadrupole doublets (no. 1 and 2 in Fig. 1) with rather similar IS values but distinctly different QS values. Doublet no. 2 represents the Fe^{2+} octahedra most altered due to metamictization process. The Mössbauer spectrum of GSP sample can be fitted by one slightly broadened Fe^{2+} quadrupole doublet (Fig. 1, Table 2). Mössbauer measurement and XRD indicate that the GSP specimen represents intermediate state between the crystalline and metamict phase of gadolinite. The GYT-CR Mössbauer spectrum was obtained after 24 h-annealing in argon at 1373 K of the GYT fragment. After heating in argon, the full crystalline structure of GYT is restored (Fig. 1). In contrast to amorphous state, the Mössbauer spectrum of the crystalline state of gadolinite (GYT-CR) can be fitted by one asymmetric quadrupole doublet. On the basis of the ^{57}Fe hyperfine parameters IS = 1.041 and QS = 1.680 mm/s (Table 2), this doublet is assigned to Fe^{2+}. In other words, Fe^{2+} cations anew occupy exactly one highly distorted octahedral site. The asymmetry of the absorption peaks is due to the Goldanski-Karyganin effect from anisotropic vibrations of Fe^{2+} in the crystalline structure of gadolinite that is confirmed by crystallographic data obtained by Miyawaki *et al.* [8].

The most notable aspect of the Mössbauer spectra (Fig. 1) is the change in the amplitudes ratio of high energy peak to low energy peak $(B - I_H)/(B - I_L)$ [6] from the Fe^{2+} components (Fig. 3) relative to the absorbed α-dose (equivalent of crystallinity). Using notation $R = (B - I_H)/(B - I_L)$, the fitting function $R(D)$ to the data corresponding GYT, GSPKM, GZI and GYT-CR (Fig. 3) can be expressed as:

$$R(D) = R_0 + A\exp\left(-\frac{D}{C}\right) \tag{2}$$

where: D is the α-decay/mg, R_0 = 0.75(3), A = 0.49(5), $C = 1.87(42) \times 10^{15}$.

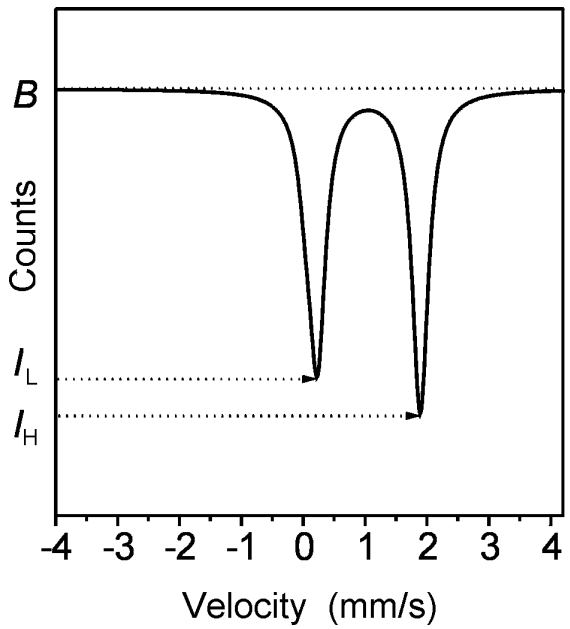

Fig. 2. Explanation of experimental parameter $(B - I_H)/(B - I_L)$ used to described evolution of Mössbauer spectra of examined gadolinites: B – mean value off-resonance counting rate; I_H, I_L – values of the counting rate in the area of maximum absorption to the high-energy and low-energy peaks for Fe^{2+} components.

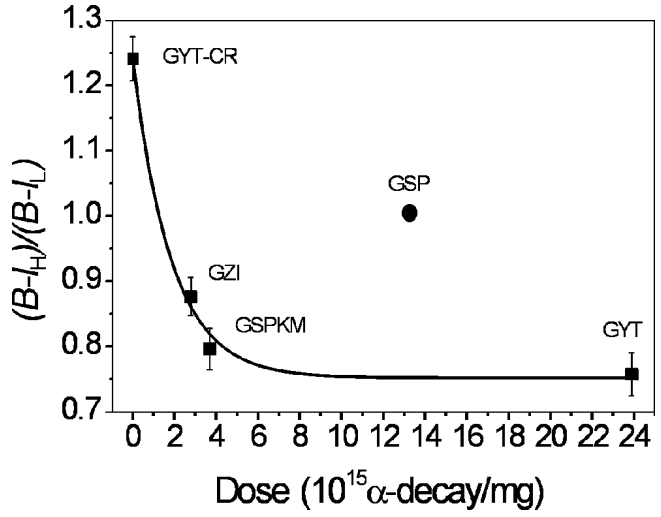

Fig. 3. Plots of $(B - I_H)/(B - I_L)$ *vs*. α-dose *D*. The solid line is the fitting function Eq. (2) to the data representing GYT, GSPKM, GZI and GYT-CR derived from a least-squares procedure.

The point corresponding to GSP (solid circle in Fig. 3) is in conflict with the estimated radiation dose based on age and the value of $(B - I_H)/(B - I_L)$ parameter and in the same way with the degree of metamictization. Since the amorphization of gadolinite occurs after doses ranging from 4 to 4.5×10^{15} α-decay events/mg [5], the GYT sample should be completely metamict. However, it is not the case. Either the age of GSP is younger than assumed for calculation, or the radiation damage in the sample was naturally annealed. Since the GSP has the same localization as GSPKM it seems that it has been subject to high-temperature hydrothermal processes, which caused high-temperature recrystallization. Generally, the function $R(D)$ can be useful for determination of metamict stage of any other gadolinite sample from Mössbauer spectroscopy.

Conclusions

The different metamict stages of gadolinite can be inferred from changes in the spectra parameter $(B - I_H)/(B - I_L)$ for divalent iron components. This parameter is a sensitive indicator of the metamictization stages of the examined gadolinite samples, which is confirmed by X-ray diffraction. The work leads to the possibility of using ^{57}Fe Mössbauer spectroscopy as a tool for rapid assessment of the metamict stage of other iron-bearing metamict minerals.

Acknowledgments The author thanks an unknown reviewer for critical comments that improved the final version of this paper.

References

1. Ewing RC (1994) The metamict state: 1993 – the centennial. Nucl Instrum Meth Phys Res B 91:22–29
2. Ewing RC, Haaker RF (1980) The metamict state: Implication for radiation damage in crystalline waste form. Nucl Chem Waste Management 1:51–57
3. Ito J, Hafner SS (1974) Synthesis and study of gadolinites. Am Mineral 59:700–708
4. Janeczek J, Eby RK (1993) Annealing in radiation damage in allanite and gadolinite. Phys Chem Miner 19:343–356
5. Malczewski D (1999) ^{57}Fe Mössbauer spectroscopy of the thermally recrystalized fully metamict gadolinites. Ph.D. Thesis. University of Silesia, Katowice, Poland
6. Malczewski D, Janeczek J (2002) Activation energy of annealed metamict gadolinite from ^{57}Fe Mössbauer spectroscopy. Phys Chem Miner 29:226–232
7. Meldrum A, Boatner LA, Weber WJ, Ewing RC (1998) Radiation damage in zircon and monazite. Geochim Cosmochim Acta 62:2509–2520
8. Miyawaki R, Nakai I, Nagashima K (1984) A refinement of the crystal structure of gadolinite. Am Mineral 69:984–953
9. Nakai I, Akimoto J, Imafuku M, Miyawaki R, Sugitani Y (1987) Characterization of the amorphous state in metamict silicates and niobates by EXAFS and XANES analyses. Phys Chem Miner 15:113–124
10. Romer RL, Smeds SA (1994) Implications of U-Pb ages of columbite-tantalites from granitic pegmatites for the Palaeoproterozoic accretion of 1.90–1.85 Ga magmatic arcs to the Baltic Shield. Precambrian Res 67:141–158
11. Pin Ch, Mierzejewski MP, Duthou JL (1987) Age of Karkonosze Mts. granite dated by isochrome Rb/Sr and its initial ^{87}Sr/^{86}Sr value. Przegląd Geologiczny 10:512–517 (in Polish)
12. Pin Ch, Puziewicz J, Duthou JL (1989) Ages and origin of a composite granitic Strzegom–Sobótka Massif, W. Sudetes (Poland). N Jb Miner Abh 160:71–82
13. Rancourt DG, Ping JY (1991) Voigt-based methods for arbitrary-shape static hyperfine parameter distributions in Mössbauer spectroscopy. Nucl Instrum Meth Phys Res B 58:85–97
14. Weber WJ, Ewing RC, Catlow CRA *et al.* (1998) Radiation effects in crystalline ceramics for the immobilization of high-level nuclear waste and plutonium. J Mater Res 13:1434–484